Anisotropic Terahertz Dynamics of Highly-Aligned Single-Walled Carbon Nanotubes

L. Ren[1], C. L. Pint[2], A. K. Wójcik[3], T. Arikawa[1], Y. Takemoto[4], K. Takeya[4], I. Kawayama[4], A. A. Belyanin[3], M. Tonouchi[4], R. H. Hauge[2], and J. Kono[1*]
[1]Department of Electrical and Computer Engineering, Rice University, Houston, Texas 77005, USA
[2]Department of Chemistry, Rice University, Houston, Texas 77005, USA
[3]Department of Physics, Texas A&M University, College Station, Texas 77843, USA
[4]Institute of Laser Engineering, Osaka University, Yamadaoka 2-6, Suita, Osaka 565-0871, Japan
* Email: kono@rice.edu

Abstract: This paper summarizes our recent advances in the spectroscopy of single-walled carbon nanotubes (SWNTs) in the terahertz (THz) range. Using polarization-dependent time-domain THz spectroscopy, we have studied the anisotropic conduction properties of free carriers in a thin film of highly aligned SWNTs. When the THz polarization was parallel to the nanotube alignment direction, there was strong absorption, while virtually no absorption was observed when the THz polarization was perpendicular to the nanotube axis. Through a proper model, the THz complex dynamic conductivity of the SWNTs was extracted and showed a non-Drude-like frequency dependence, with the real part monotonically increasing with increasing frequency and exhibiting a peak around 4.5 *THz*. Furthermore, the reduced linear dichroism was calculated to be 3, which demonstrates the nematic order parameter to be 1. This indicates that the alignment of the nanotubes is "perfect" and any misalignment must have characteristic length scales much smaller than the wavelengths used in these experiments (1.5 *mm* – 150 μm).

Keywords: Terahertz spectroscopy, carbon nanotubes, dynamic conductivity, anisotropy

1. Introduction

Single-walled carbon nanotubes (SWNTs) represent one of the most direct realizations of a one-dimensional (1-D) electron system available today. Since their discovery in 1993 [1,2], their exotic physical, chemical, and mechanical properties have been extensively studied [3-5]. They are one of the leading candidate technologies to unify electronic and optical functions in nanoscale circuits. At the same time, they provide ideal model 1-D condensed matter systems in which to address fundamental theoretical questions in many-body physics.

A number of experimental THz / far-infrared (FIR) spectroscopic studies have been performed over the last decade on SWNTs of various forms [6-15], producing an array of conflicting results with contradicting interpretations. This is partly due to the widely differing types of samples used in these studies – grown by different methods (HiPco, CoMoCAT, CVD, and laser ablation) and put in a variety of polymer films that are transparent in the THz range. Nanotubes in most of these samples were bundled and typically consist of a mixture of semiconducting and metallic nanotubes with a wide distribution of diameters. Some of the samples used were partially aligned through mechanical stretching, showing some degree of anisotropy in their THz response [9,10,12]. One common spectral feature that many groups have detected is an absorption peak around 135 cm^{-1} (or ~4 *THz* or ~17 *meV*). This feature, first observed by Ugawa et al. [7] in the real part of the conductivity, has been interpreted as interband absorption in metallic (or mod 3) nanotubes with curvature-induced gaps [7,14,15] or absorption due to classical plasmon oscillations along the tube axis [12], but a consensus has not been achieved.

In this paper, we review our recent work on the dynamic (also known as the AC or optical or frequency (ω) dependent) conductivity σ(ω) of SWNTs. Much information on carrier states and dynamics in metals can be obtained through such measurements. The classical Drude formula $\sigma(\omega) = \sigma(0)/(1-i\omega\tau)$ (where τ is the momentum relaxation time), which works well for ordinary metals at room temperature, is expected to fail when electron-electron interactions or disorder (or both) is a significant perturbation to the unperturbed single-particle states. Many-body effects can affect the temperature (T) and magnetic field (B) dependences of the conductivity σ(ω,T,B), sometimes in very specific ways, making this a very useful method for comparing with theoretical calculations. In particular, we have observed strongly anisotropic THz response of highly-aligned SWNTs. There was virtually no attenuation (strong absorption) when the THz polarization was perpendicular (parallel) to the nanotube axis. The dynamic complex dielectric conductivity tensor elements were determined, and the real part of the parallel conductivity showed a non-Drude-like frequency dependence.

2. Experimental Methods

The films of highly-aligned SWNTs used in this study were fabricated using the methods described in Ref. [16]. The as-grown lines of aligned SWNTs initially adopt a vertical orientation with respect to the growth substrate, with a length determined by the growth duration. Following the growth process, a high temperature (750°C) H_2O vapor etch was employed to free the catalyst-SWNT interface, allowing efficient transfer of an aligned film to a host substrate of choice (sapphire in our case). This transfer method relies on the simple concept of strong side-wall van der Waals adhesion between SWNTs and the transfer substrate, and weaker SWNT-end interaction with the growth substrate. This is analogous to the mechanism behind the "Gecko" effect [17]. The result of the transfer process is a homogenous film (initially ~2 μm thick) that remains as-grown, highly aligned, and free of exposure to any sort of solvent or liquid. Fig. 1 shows scanning electron microscope images of the SWNT alignment present in such a transferred film, emphasizing the high degree of alignment, which makes this film well-suited for the study presented in this work.

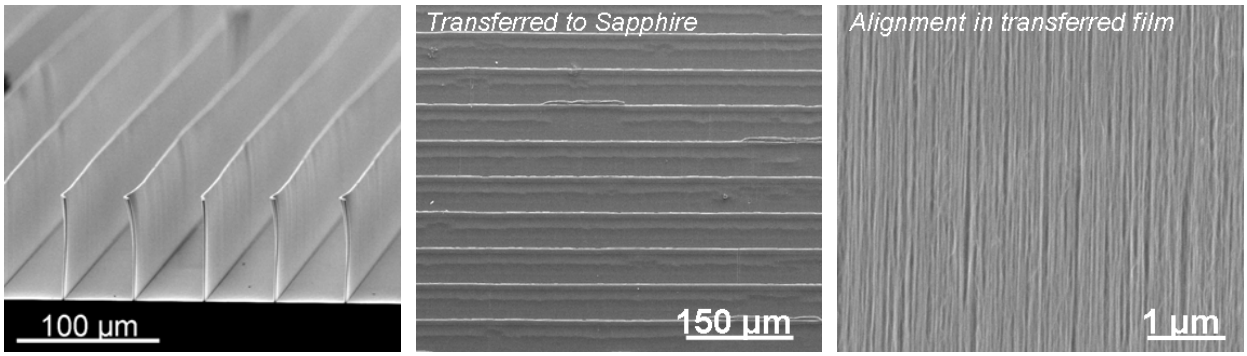

Fig. 1 Scanning electron microscope images of highly-aligned single-walled carbon nanotubes on the growth substrate (left) and after a transfer to the sapphire substrate (middle, right). The nanotubes are vertically aligned on the growth substrate, while they are horizontally aligned on the sapphire substrate. The length of the nanotubes is very uniform and determined by the growth duration.

We used two THz setups in this study. The main THz setup we utilized was a typical time-domain THz spectroscopy system based on photoconductive antennas, where both the THz

emitter and detector were made of low-temperature grown GaAs [18,19]. The THz beam obtained from such an emitter was already highly linearly polarized, but a free standing wire-grid polarizer with a degree of polarization of more than 99.5% in this range was placed in the path of the incident THz beam (8 inches both from the emitter and sample) to ensure the high degree of polarization of the THz beam incident on the sample. The second THz system we employed had a DAST crystal as the emitter, which extended the usable frequency range to ~5 *THz*. As schematically shown in the inset of Fig. 2, the SWNT sample was rotated about the propagation direction of the THz wave, which changed the angle, θ, between the nanotube axis and the THz electric field polarization direction from 0° to 90°. Thus, polarization-dependent THz transmission measurements were performed on both the SWNT film sample on a sapphire substrate and a reference sapphire sample with the same thickness as the sample substrate.

3. Experimental Results and Discussion

Fig. 2 shows transmitted time-domain waveforms for four different angles (θ = 0°, 30°, 45°, and 90°), together with the waveform transmitted through a reference sapphire substrate with no nanotubes (dashed line with open circles). Note that the 90-degree trace precisely coincides with the reference waveform, indicating that there is no attenuation by going through the film when the polarization is perpendicular to the nanotube alignment direction. When θ = 0° (parallel polarization), on the other hand, the THz wave is strongly absorbed by the nanotubes.

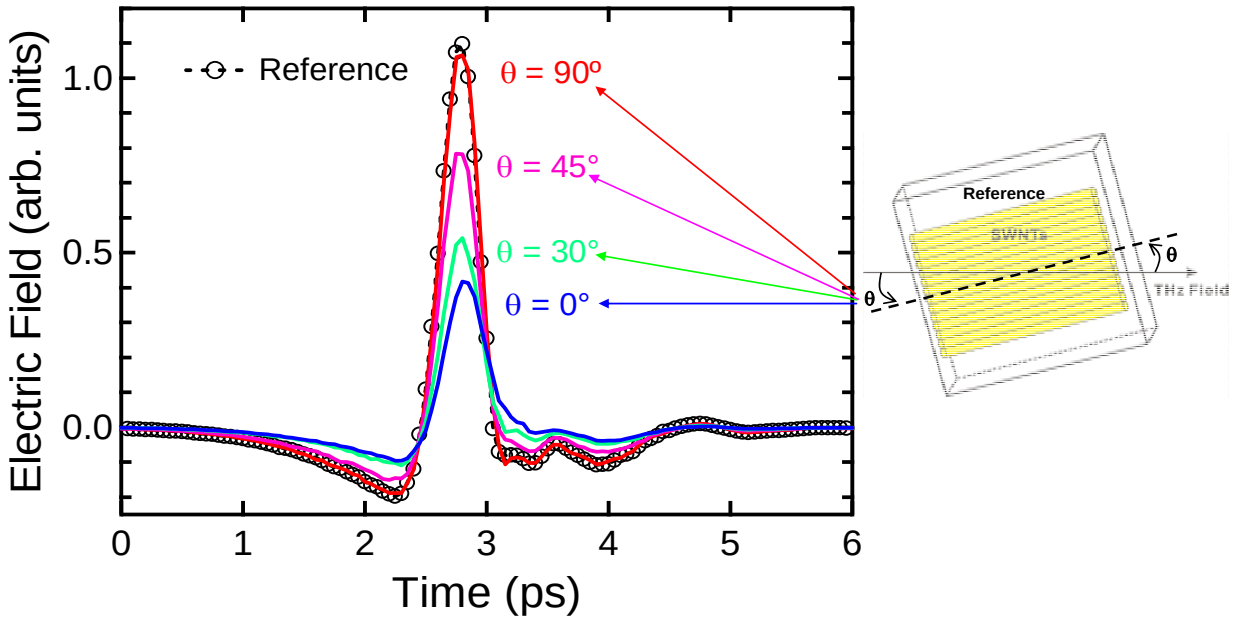

Fig. 2 Transmitted THz electric field signals for the reference sapphire substrate (dashed curve with circles) and for the nanotube film for different polarization angles (colored solid curves). The THz wave is most strongly attenuated when the THz polarization is parallel to the tube alignment direction (θ = 0°), whereas there is no attenuation within the experimental accuracy for the perpendicular case (θ = 90°).

Strongly anisotropic THz absorption is better seen in the frequency domain after Fourier-transforming the time-domain waveforms and calculating absorbance spectra, as shown

in Fig. 3. Here, we plot the absorbance, $A = -\mathrm{Log}_{10}(T)$, as a function of frequency in the 0.2-1.8 *THz* range, where T is the transmittance defined as $T = |E_s/E_r|^2$ and E_s and E_r are the complex THz signals in the frequency domain for the sample and reference, respectively. From this figure, we can clearly see that as the angle θ increases from 0° to 90°, the absorbance of the SWNTs decreases monotonically. When θ = 90°, the absorbance is zero throughout this frequency range. On the other hand, when θ = 0°, the absorbance is finite and high; it increases with increasing frequency, reaching a value over 1.0 at 1.8 THz. The 30° and 45° absorbance lines show the same trend as the 0° curve but with smaller amplitudes.

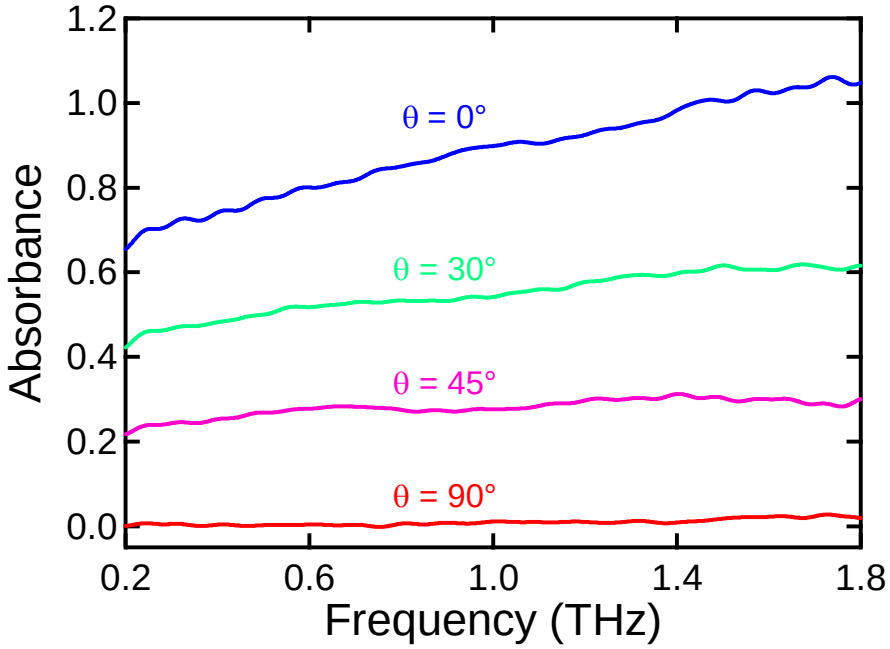

Fig. 3 THz absorbance spectra for the SWNT film for four different polarization angles. As the angle between the THz polarization and nanotube alignment direction increases, the absorbance monotonically increases.

In order to quantify the degree of alignment of SWNTs in this film from these THz transmission data, we employ a data analysis procedure developed for studying anisotropic optical properties of SWNTs in the optical range [20]. Fig. 4(a) plots the parallel ($A_{//}$) and perpendicular ($A_{\perp}$) absorbance spectra, corresponding to θ = 0° and 90°, respectively. Also plotted in Fig. 4(a) is the isotropic absorbance defined as $A_0 \equiv (A_{//} + 2A_{\perp})/3$, which represents the absorbance expected if the nanotubes were randomly oriented [20]. Finite alignment moves up (down) $A_{//}$ ($A_{\perp}$) with respect to A_0 and induces a finite linear dichroism, $LD = A_{//} - A_{\perp}$, shown in Fig. 4(b). However, it is the reduced linear dichroism, $LD^r \equiv LD/A_0$, that provides a normalized measure of alignment. For example, LD increases with the film thickness, while LD^r remains the same. From a microscopic viewpoint, the LD^r can be expressed as

$$LD^r = 3[(3\cos^2\alpha - 1)/2]\cdot S, \quad (1)$$

where α is the angle between the long axis and the direction of the dipole moment and S is the nematic order parameter (= 0 when the nanotubes are randomly oriented and = 1 when the nanotubes are perfectly aligned). Fig. 4(b) indicates that within our experimental range LD^r is nearly constant at 3, which, combined with Eq. (1), indicates that S ~ 1, assuming that α = 0.

Note that any finite value of α would result in a value of S that is larger than 1, which is impossible by definition. Therefore, the fact that $LD^r \sim 3$ proves not only that the nanotubes are well aligned (S ~ 1) but also that the THz response of SWNTs is intrinsically anisotropic (α ~ 0). Finally, as an important parameter for a polarizer, we calculated the degree of polarization, $P = (A_{//} - A_{\perp})/(A_{//} + A_{\perp})$, which is plotted in Fig. 4(c). As shown, it is very close to 1 throughout the entire frequency region. All of these data suggest that this THz polarizer is of excellent quality.

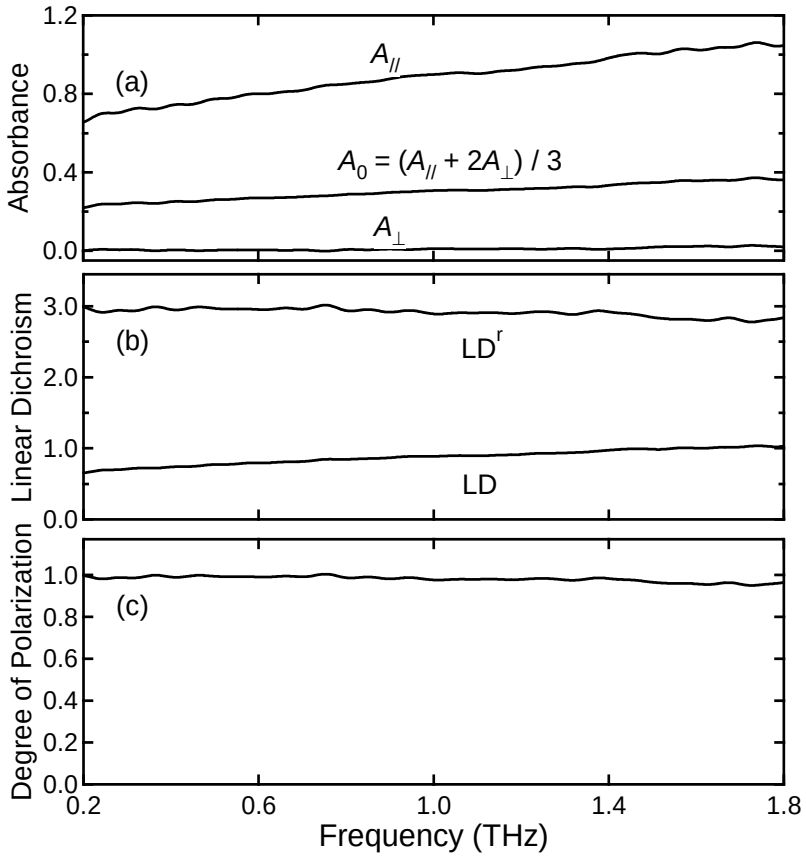

Fig. 4 (a) Parallel ($A_{//}$), perpendicular ($A_{\perp}$), and isotropic (A_0) absorbance, (b) linear dichroism (*LD*) and reduced linear dichroism (LD^r), and (c) degree of polarization (DOP) as a function of frequency, measured for the aligned SWNT film.

The increasing absorbance with frequency in this spectral range is consistent with previous far-infrared spectroscopy results on various types of SWNT samples showing a robust absorption peak around 4 *THz,* whose origin is not understood [7-15]. The dynamic complex conductivity tensor elements, extracted from our data, are shown in Fig. 5. Again, extremely anisotropic responses are observed. At 90°, when the THz polarization is perpendicular to the nanotube axis, the real part of the conductivity is zero, showing no sign of absorption. This should be contrasted to the 0° case, when the THz polarization is parallel with the nanotubes, the conductivity is ~ 80 $S \cdot cm^{-1}$ at 1.8 *THz*. In addition, the dynamic conductivity shows a non-Drude frequency dependence, with the real part monotonically increasing with increasing frequency between 0.2 *THz* and 1.8 *THz*. Furthermore, we made additional measurements using a THz-TDS system based on a DAST crystal to extend the frequency range up to ~5 THz and observed a peak at ~4 *THz*, as shown in the inset of Fig. 5(left).

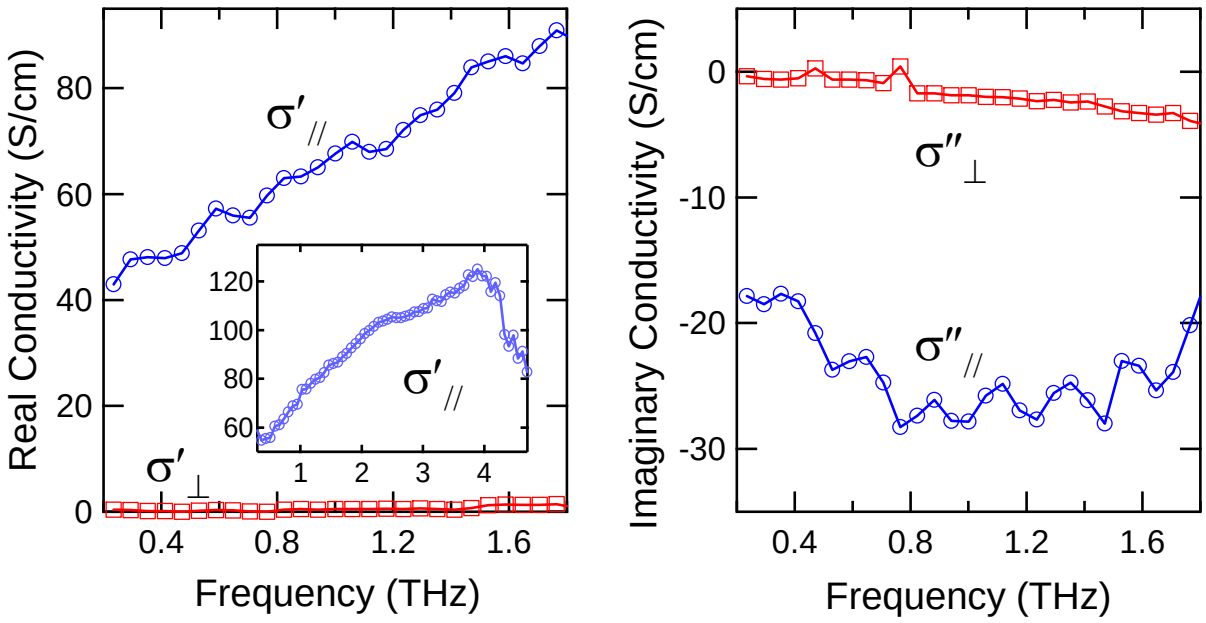

Fig. 5 (a) Real and (b) imaginary parts of parallel and perpendicular elements of the dynamic conductivity tensor for the aligned SWNT film extracted from the THz time-domain signals. Inset: Real part of the parallel and perpendicular elements of the dynamic conductivity tensor for the aligned SWNT film up to ~5 *THz* extracted from data taken with a DAST-based THz time-domain spectroscopy setup.

4. Conclusions

Terahertz time-domain spectroscopy of a highly-aligned single-walled carbon nanotube film reveals strongly anisotropic responses. The deduced complex dynamic conductivity clearly showed a non-Drude-like frequency dependence, with the real part showing a peak at ~ 4 *THz*.

Acknowledgement

This work was supported by the National Science Foundation (through Grant No. OISE-0530220), the Department of Energy (through Grant No. DEFG02-06ER46308), and the Robert A. Welch Foundation (through Grant No. C-1509).

References

[1] S. Iijima and T. Ichihashi, "Single-Shell Carbon Nanotubes of 1-nm Diameter," *Nature* 363, 603, (1993).

[2] D. S. Bethune, C. H. Klang, M. S. de Vries, G. Gorman, R. Savoy, J. Vazquez, and R. Beyers, "Cobalt-Catalysed Growth of Carbon Nanotubes with Single-Atomic-Layer Walls," *Nature* 363, 605, (1993).

[3] R. Saito, G. Dresselhaus, and M. S. Dresselhaus, *Physical Properties of Carbon Nanotubes,* Imperial College Press, London, (1998).

[4] M. S. Dresselhaus, G. Dresselhaus, and P. Avouris, editors, *Carbon Nanotubes: Synthesis, Structure, Properties, and Applications*, no. 18 in Topics in *Applied Physics*, Springer, Berlin, (2001).

[5] A. Jorio, G. Dresselhaus, and M. S. Dresselhaus, editors, *Carbon Nanotubes: Advanced Topics in the Synthesis, Structure, Properties and Applications,* Springer, Berlin, (2008).

[6] F. Bommeli, L. Degiorgi, P. Wachter, W. S. Bacsa, W. A. de Heer, and L. Forro, "Evidence of Anisotropic Metallic Behavior in the Optical Properties of Carbon Nanotubes," *Solid State Commun.* 99, 513, (1996).

[7] A. Ugawa, A. G. Rinzler, and D. B. Tanner, "Far-Infrared Gaps in Single-Wall Carbon Nanotubes," *Phys. Rev. B* 60, R11305, (1999).

[8] M. E. Itkis, S. Niyogi, M. E. Meng, M. A. Hamon, H. Hu, and R. C. Haddon, "Spectroscopic Study of the Fermi Level Electronic Structure of Single-Walled Carbon Nanotubes," *Nano Lett*. 2, 155, (2002).

[9] T.-I. Jeon, K.-J. Kim, C. Kang, S.-J. Oh, J.-H. Son, K. H. An, D. J. Bae, and Y. H. Lee, "Terahertz Conductivity of Anisotropic Single Walled Carbon Nanotube Films," *Appl. Phys. Lett.* 80, 3403, (2002).

[10] T.-I. Jeon, K.-J. Kim, C. Kang, I. H. Maeng, J.-H. Son, K. H. An, J. Y. Lee, and Y. H. Lee, "Optical and Electrical Properties of Preferentially Anisotropic Single-Walled Carbon-Nanotube Films in Terahertz Region," *J. Appl. Phys.* 95, 5736, (2004).

[11] T.-I. Jeon, J.-H. Son, K. H. An, Y. H. Lee, and Y. S. Lee, "Terahertz Absorption and Dispersion of Fluorine-Doped Single-Walled Carbon Nanotube," *J. Appl. Phys.* 98, 034316, (2005).

[12] N. Akima, Y. Iwasa, S. Brown, A. M. Barbour, J. Cao, J. L. Musfeldt, H. Matsui, N. Toyota, M. Shiraishi, H. Shimoda, and O. Zhou, "Strong Anisotropy in the Far-Infrared Absorption Spectra of Stretch-Aligned Single-Walled Carbon Nanotubes," *Adv. Mater.* 18, 1166, (2006).

[13] F. Borondics, K. Kamarás, M. Nikolou, D. B. Tanner, Z. H. Chen, and A. G. Rinzler, "Charge Dynamics in Transparent Single-Walled Carbon Nanotube Films from Optical Transmission Measurements," *Phys. Rev. B* 74, 045431, (2006).

[14] H. Nishimura, N. Minami, and R. Shimano, "Dielectric Properties of Single-Walled Carbon Nanotubes in the Terahertz Frequency Range," *Appl. Phys. Lett.* 91, 011108, (2007).

[15] T. Kampfrath, K. von Volkmann, C. M. Aguirre, P. Desjardins, R. Martel, M. Krenz, C. Frischkorn, M. Wolf, and L. Perfetti, "Mechanism of the Far-Infrared Absorption of Carbon-Nanotube Films," *Phys. Rev. Lett.* 101, 267403, (2008).

[16] C. L. Pint, Y.-Q. Xu, M. Pasquali, and R. H. Hauge, "Formation of Highly Dense, Aligned Ribbons and Ultra-thin Films of Single-Walled Carbon Nanotubes from Carpets," *ACS Nano* 2, 1871, (2008).

[17] L. Qu, L. Dai, M. Stone, Z. Xia, and Z. L. Wang, "Carbon Nanotube Arrays with Strong Shear Binding-On and Easy Normal Lifting-Off," *Science* 322, 238, (2008).

[18] X. Wang, D. J. Hilton, L. Ren, D. M. Mittleman, J. Kono, and J. L. Reno, "Terahertz Time-Domain Magnetospectroscopy of a High-Mobility Two-Dimensional Electron Gas," *Optics Lett.* 32, 1845, (2007).

[19] L. Ren, C. L. Pint, L. G. Booshehri, W. D. Rice, X. Wang, D. J. Hilton, K. Takeya, I. Kawayama, M. Tonouchi, R. H. Hauge, and J. Kono, "Carbon Nanotube Terahertz Polarizer," *Nano Lett.* 9, 2610, (2009).

[20] See, e.g., J. Shaver, A. N. G. Parra-Vasquez, S. Hansel, O. Portugall, C. H. Mielke, M. von Ortenberg, R. H. Hauge, M. Pasquali, and J. Kono, "Alignment Dynamics of Carbon Nanotubes in Pulsed Ultrahigh Magnetic Fields," *ACS Nano* 3, 131, (2009).